On the sea water corrosion resistance of Alloy 825 CTP (UNS N08827), an improved version of Alloy 825 (UNS N08825)

Julia Botinha
VDM Metals International GmbH
Kleffstraße 23
58762 Altena
Germany

Philipp Huebner
VDM Metals International GmbH
Kleffstraße 23
58762 Altena
Germany

Katharina Utens
RWTH Aachen University
Intzestraße 5
52072 Aachen
Germany

Daniela Zander
RWTH Aachen University
Intzestraße 5
52072 Aachen
Germany

Helena Alves
VDM Metals International GmbH
Kleffstraße 23
58762 Altena
Germany

ABSTRACT

UNS[1] N08827, commercially called Alloy 825 CTP[2], represents a significant advancement of UNS N08825 (Alloy 825)[2] by virtue of its tailored chemical composition, resulting in enhanced localized corrosion resistance. The key modification in UNS N08827 involves a notable augmentation in molybdenum content, which has been raised to approximately 6%, twice the amount found in the conventional UNS N08825, which contains 3% molybdenum. Consequently, this alloy surpasses a critical threshold for the pitting resistance equivalent number (PREN) by exceeding 40, a prerequisite for specific applications within the oil and gas sector.

Prior investigations have already demonstrated the heightened resistance of UNS N08827 to pitting and crevice corrosion when exposed to ferric chloride solutions, as evidenced by ASTM[3] G48 C and D tests. Building upon this foundation, the subsequent objective was to assess the corrosion performance of this alloy in an artificial seawater environment. This research paper presents the outcomes obtained from

---

[1] Unified Numbering System

[2] Trade name

[3] American Society for Testing and Materials, West Conshohocken, Pennsylvania, USA

subjecting Alloy 825 CTP UNS N08827 to ASTM G61 and ASTM G150 tests, focusing on its corrosion behavior.

Key words: Corrosion resistant alloys, Nickel alloys, Pitting, Seawater corrosion

INTRODUCTION

UNS N08827 has been introduced to the market in the last years as an alternative alloy for use in the oil and gas industry. This alloy has been engineered to bridge the existing gap in localized corrosion resistance between two other well known alloys, namely Alloy 825 (UNS N08825) and Alloy 625 (UNS N06625). The main chemical composition of the three alloys is given on Table 1.[1]

Table 1: Main chemical composition of UNS N08825, UNS N08827 and UNS N06625

Alloy	Ni	Cr	Fe	C	Cu	Ti	Mo	Nb
825 (UNS N08825)	38.0-46.0	19.5-23.0	R	Max 0.05	1.5-3.0	0.6-1.2	2.5-3.5	-
825 CTP (UNS N08827)	39.0-43.0	21.0-23.0	R	Max 0.015	1.6-4.0	Max 0.10	4.5-6.5	-
625 (UNS N06625)	58-71	21-23	Max 5	Max 0.03	-	Max 0.4	8-10	3.2-3.8

UNS N08827 is characterized as a solid-solution nickel alloy, possessing a chemical composition closely resembling that of the traditional UNS N08825, with the notable exception of having absence of titanium and double the molybdenum content.

In the 1950s,[2] the development of UNS N08825 coincided with manufacturing limitations that constrained the attainment of low carbon levels achievable today. In response, elements such as titanium and niobium were commonly introduced into solid solution alloys to stabilize carbon and avert the precipitation of chromium carbides alongside the grain boundaries. These carbides have the capacity to sequester chromium within the alloy matrix, leading to chromium depletion near their precipitation sites, namely the grain boundaries, rendering the alloys susceptible to intergranular corrosion attack.

The composition specifications for UNS N08825 stipulate a minimum of 0.6 wt.-% titanium with the intention of limiting sensitization due to carbide precipitation as described above. However, the presence of titanium poses challenges in terms of weldability. Titanium exhibits a significant affinity not only for carbon, as previously discussed, but also for nitrogen, resulting in the formation of titanium nitrides. Although the available literature offers limited insight into the influence of titanium on the weldability of nickel alloys, some authors have documented its effects.[3,4,5] The advantage of the absence of titanium in UNS N08827 has been discussed in recent publications.[6]

Another heightened change in UNS N08827 is the molybdenum content, which ranges from 4.5 to 6.5 % and imparts superior localized corrosion resistance to UNS N08827 when compared to UNS N08825 that typically contains molybdenum within the range of 2.5 to 3.5%. This enhanced resistance is particularly evident in environments containing chloride. This property is well-documented and quantified through the utilization of the Pitting Resistance Equivalent Number (PREN), as defined by

$$PREN = 1 \times \%Cr + 3.3 \times (\%Mo + 0.5 \times \%W) + 16 \times \%N \ .$$

The improved localized resistance acquired by UNS N08827 by means of increased molybdenum content has been experimentally confirmed earlier by means of the application of ASTM G48[7] Methods C and D tests.[3] These well known immersion tests were used to determine the Critical Pitting Temperature (CPT) and Critical Crevice Temperature (CCT) on a solution composed by 6% $FeCl_3$ and 1% HCl. The CPT and CCT defined by these test methods are summarized on Table 2.

Table 2: Critical Pitting Temperature (CPT) and Critical Crevice Temperature (CCT) of UNS N08825 and UNS N08827 determined by means of ASTM G48 Methods C and D

Material	CPT [°C]	CCT [°C]
UNS N08827 (3)	50	20
UNS N08825 (values from literature) (8)	30	< 5

Within this investigation program, the pitting corrosion behavior of samples of UNS N08825 and UNS N08827 are investigated in iron-chloride solution as well as in the ASTM artificial seawater according to ASTM D1141-52[9] with the composition given on Table 3. Four samples per material per solution per method are investigated, totalizing 32 samples.

Table 3: Composition of artificial seawater according to ASTM D1141

Sodium Chloride	NaCl	24.53 g/L
Magnesium Chloride	$MgCl_2$ x 6 H_2O	10.1 g/L
Sodium Sulfate	Na_2SO_4	4.09 g/L
Calcium Chloride	$CaCl_2$	1.16 g/L
Potassium Chloride	KCl	0.695 g/L
Sodium Bicarbonate	$NaHCO_3$	0.201 g/L
Potassium Bromide	KBr	0.101 g/L
Boric Acid	H_3BO_3	0.027 g/L
Strontium Chloride	$SrCl_2$	0.025 g/L
Sodium Fluoride	NaF	0.003 g/L
Water	H_2O	988.968 g/L

EXPERIMENTAL PROCEDURE

The critical pitting temperatures (CPT) are determined according to ASTM G150[10] using an Avesta cell as schematized on Figure 1. Both iron-chloride solution and ASTM artificial seawater are used as electrolyte. The iron-chloride solution is used as a reference, to compare ASTM G150 test on the Avesta cell with the well-known and mill-qualification-applied ASTM G48 test. At least four specimens are cut from large-scale sheet material from each alloy and are prepared for the determination of the CPT.

During the test, a potential of 700 mV is applied and the temperature is increased with a heating rate of 1 K/min. The test is manually stopped when the current density is above 100 µA/cm^2 for 1 minute. The temperature at this point is defined as the CPT.

The advantage of using an Avesta cell lies in its design, which avoids micro crevice corrosion formed between the working electrode and the gasket at the bottom aperture of the cell. The crevice corrosion is eliminated by flooding a filter paper ring that is placed between the sample and the gasket using distilled water.
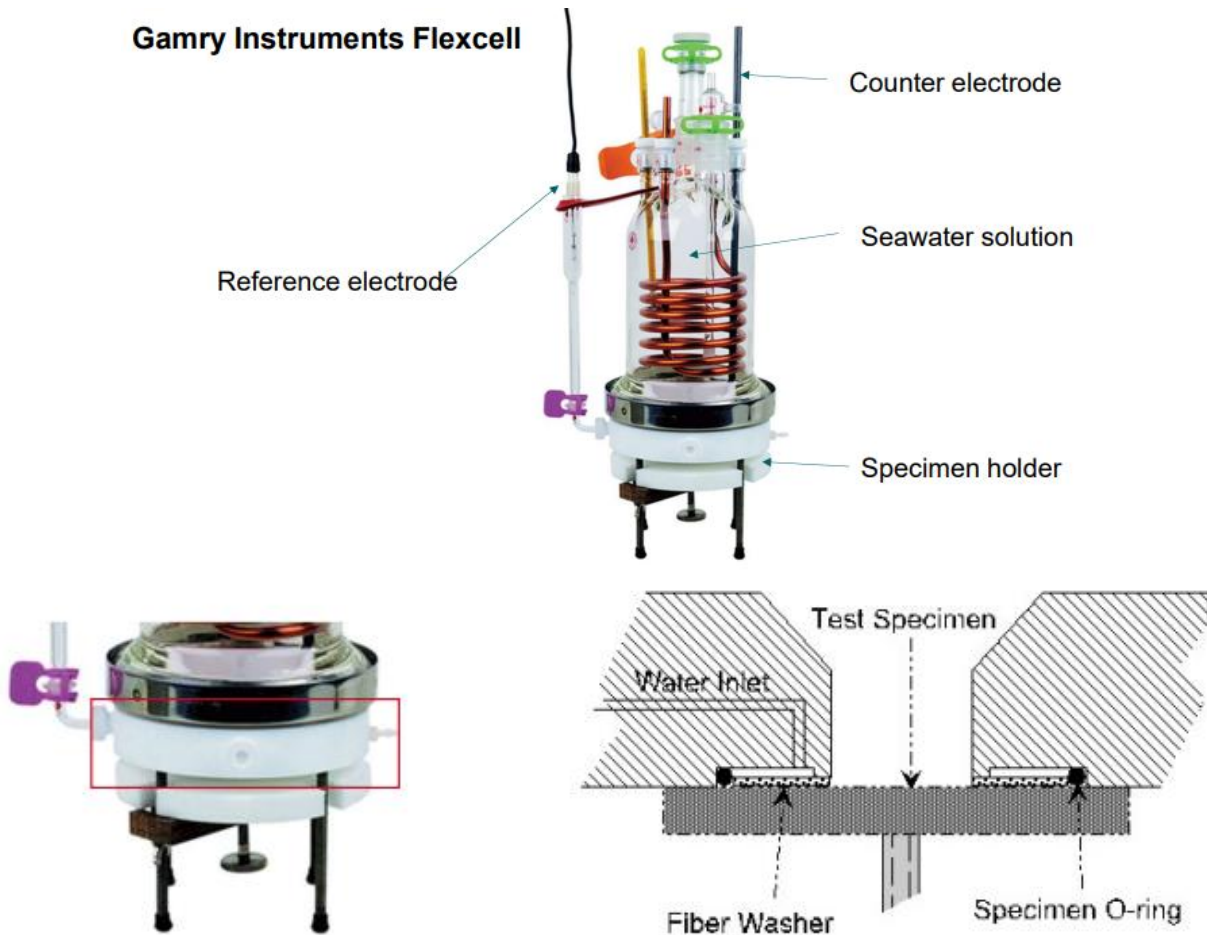
Figure 1: Scheme of Avesta cell set-up[11]

In order to investigate the passivation and breakdown behavior of both alloys, cyclic polarization tests are performed using the test set-up as represented in Figure 2 filled with 500 mL of fresh solution for each test. The reference electrode is Ag/AgCl and a platinum plate is used as counter-electrode. Specimens having a surface area of 1 cm^2 are prepared from large-scale produced sheets. Current density vs. potential curves are recorded by means of cyclic polarization measurements based on ASTM G61[12]. The flowing currents are measured via the change in potential. The measurement is performed inside of a Faradays's cage in order to avoid any external magnetic/electric influence on the measurements. The resulting corrosion current density and the corrosion potential are determined in order to compare the pitting corrosion potential of both materials at 30 °C.
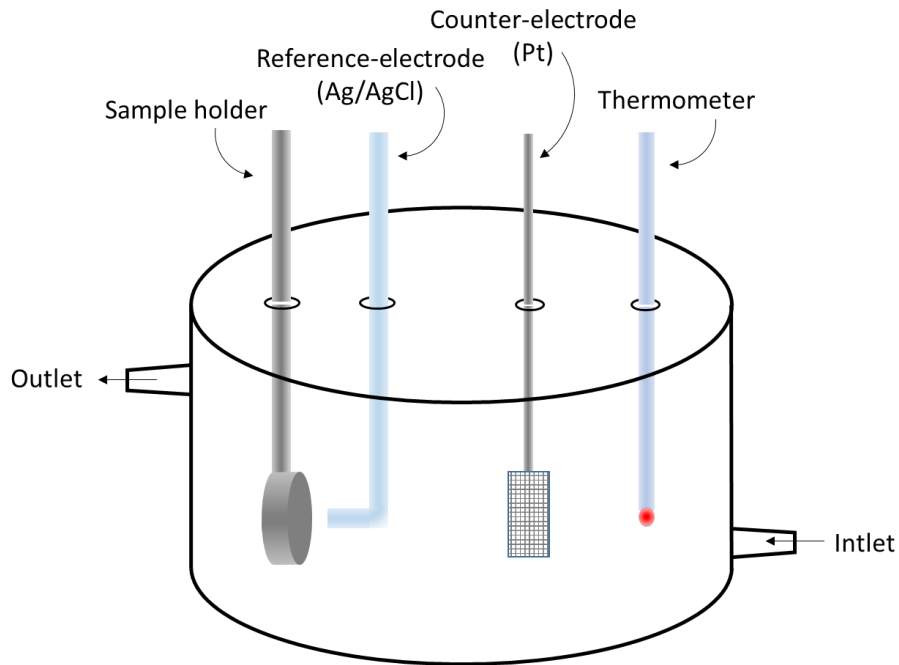
Figure 2: Test set-up for cyclic polarization tests according to ASTM G61

RESULTS

Corrosion measurements in acidified iron-chloride electrolyte

The critical pitting temperatures (CPT) determined using an Avesta Cell according to ASTM G150 on iron-chloride electrolyte are given on Table 4. Figure 3 shows the measured corrosion density with the increase of temperature. As per definition, the CPTs are the temperatures at which the corrosion densities reach 100 µA/cm^2. The UNS N08825 has a CPT of 33.6 °C in average, while in UNS N08827 the critical pitting temperature lies at 45.7 °C.

The critical pitting temperatures defined on the experiments carried out in iron-chloride electrolyte are used with the intuition of enabling a direct comparison with the ASTM G48 tests. Considering that the already published data mentions for UNS N08825 a CPT of 30 °C and for UNS N08827, a CPT of 50 °C, we consider that the Avesta values are in very good agreement with the ASTM G48 values, considering that variations could be inserted by e.g. slight chemical composition variations or sample preparation. These results confirm that UNS N08827 has an enhanced resistance to localized corrosion in iron-chloride solution compared to UNS N08825.

Table 4: Critical pitting temperatures of UNS N08825 and UNS N08827 in iron-chloride solution according to ASTM G150

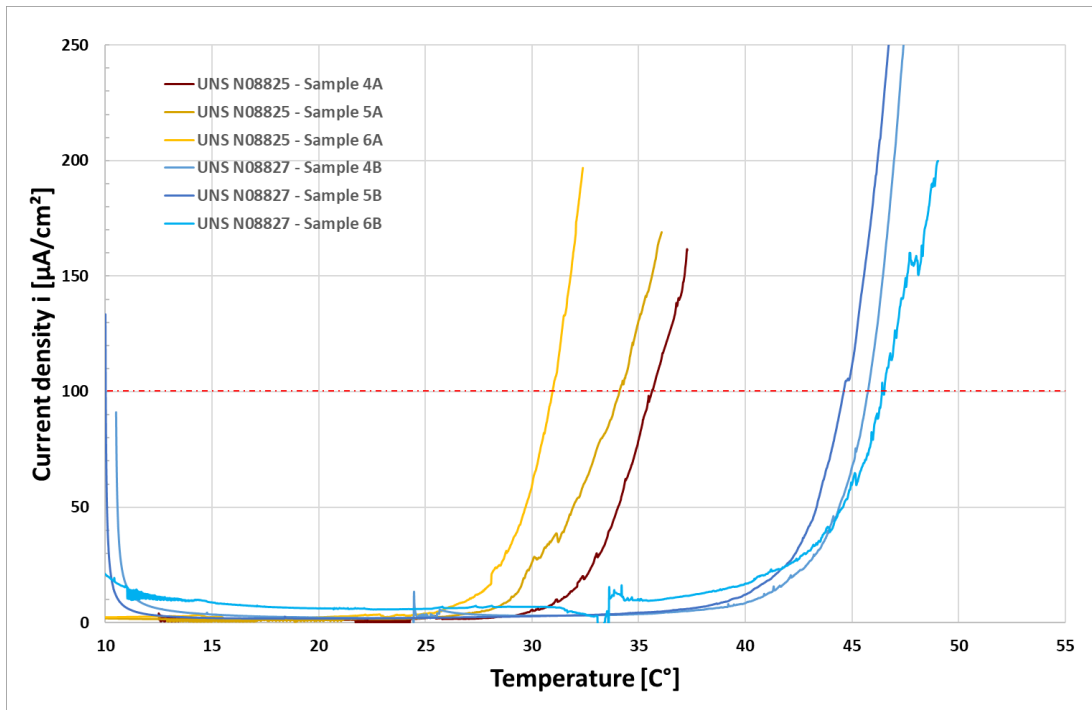| Alloy	Sample	CPT [°C]	Average CPT [°C]
UNS N08825	4A	35.2	33.6
	5A	34.6	
	6A	31.1	
UNS N08827	4B	45.8	45.7
	5B	44.7	
	6B	46.6	

Figure 3: Current density measurements of UNS N08825 and UNS N08827 during temperature increase under iron-chloride solution according to ASTM G150

Polarization curves according to ASTM G61 in iron-chloride solution at 30 °C are shown in Figure 4 and the measured pitting-potential (E_{pit}) and pitting-current density (i_{pit}) are summarized on Table 5. The breakdown potential is similar for both alloys in this solution at a temperature of 30 °C.
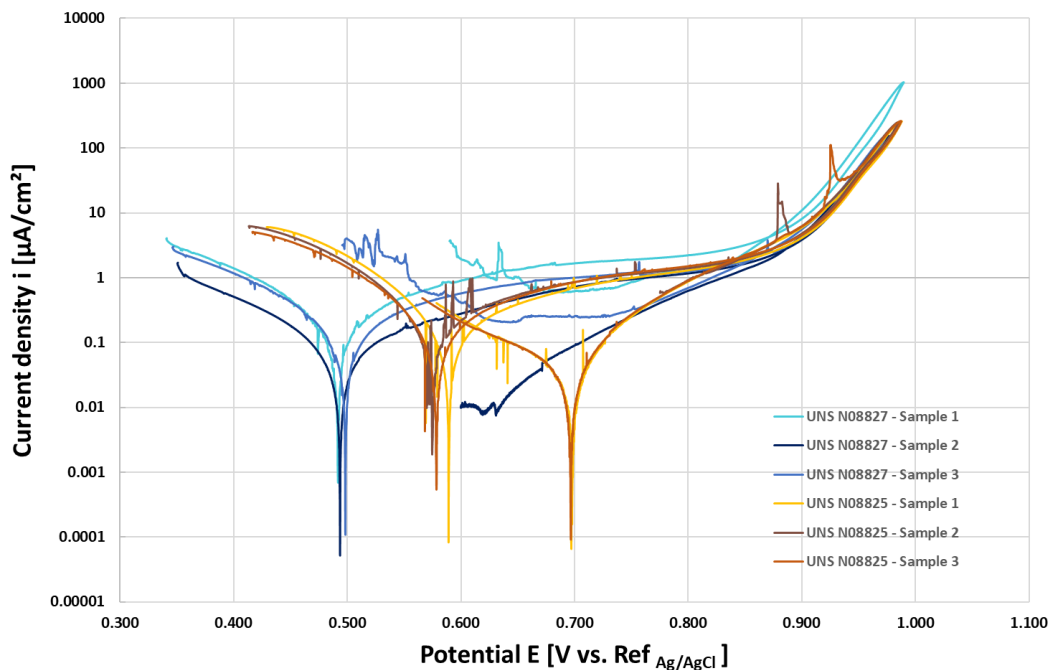

Figure 4: Cyclic potentiodynamic polarization curves of UNS N08825 and UNS N08827 in iron-chloride solution measured according to ASTM G61 at 30 °C

The open circuit potential (OCP) of UNS N08827 is slightly lower than the OCP of UNS N08825. One could argue that UNS N08827 is less stable in iron-chloride solution than UNS N08825 only based in that value, but the pitting and repassivation potentials evidence UNS N08827's corrosion resistance is at least equal to the resistance of UNS N08825 in these testing conditions. Thereby it can be concluded that UNS N08827 interacts much faster with the media, which leads to the formation of a passive layer that is kept through the testing duration until the breakdown potential is reached and is quickly re-established through repassivation.

Figure 5 is a zoom-in area of the diagrams of Figure 4 with the aim of showing the repassivation potentials of each sample. It can be observed that both alloys exhibit a short hysteresis loop, which indicates that repassivation of existing pits is possible. Nevertheless, it is noted that UNS N08827 repassivates at higher potentials compared to UNS N08825, which can be explained by its more noble chemical composition.
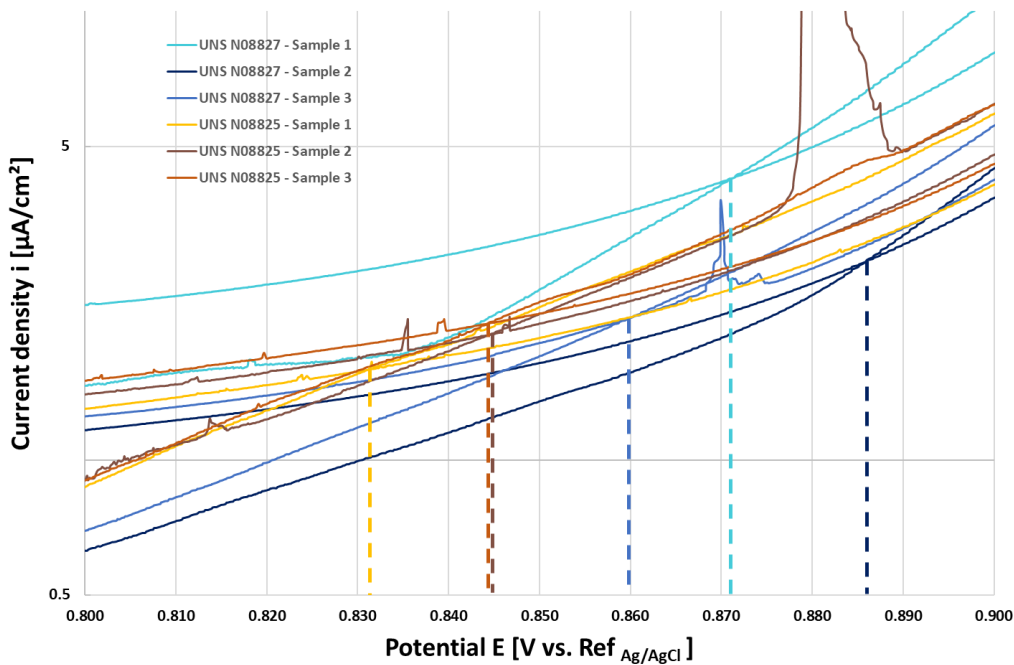

Figure 5: Zoomed cyclic potentiodynamic polarization curves of UNS N08825 and UNS N08827 in iron-chloride solution measured according to ASTM G61 at 30 °C showing repassivation potentials with dashed lines

Table 5: Pitting potential and pitting corrosion at 30 °C defined based on cyclic-pontentiodynamic polarization curves in iron-chloride solution according to ASTM G61.

Alloy	Sample	E_{pit} [$V_{(Ag/AgCl)}$]	i_{pit} [$\mu A/cm^2$]
UNS N08825	1	0.883	4.49
	2	0.887	3.56
	3	0.884	4.49
	Average	**0.885 ± 0.002**	**4.022 ± 0.47**
UNS N08827	1	0.870	4.1
	2	0.886	2.85
	3	0.872	2.52
	Average	**0.876 ± 0.009**	**3.157 ± 0.83**

Corrosion measurements in synthetic sea water electrolyte

When the Avesta experiments are carried out using artificial seawater with chemical composition according to ASTM D1141, the critical pitting temperature of both alloys is higher in comparison to ASTM G48 testing solution. The average CPT of UNS N08825 lies now at 38 °C and the CPT of UNS N08827 lies at about 58 °C, as shown on Table 6 and Figure 6.

Table 6: Critical pitting temperatures of UNS N08825 and UNS N08827 in synthetic seawater according to ASTM G150

Alloy	Sample	CPT [°C]	Average CPT [°C]
825 (UNS N08825)	1A	38.0	38.1
	2A	40.5	
	3A	35.7	
825 CTP (UNS N8827)	1B	59.1	58.1
	2B	53.6	
	3B	61.7	

These results show that the ASTM G48 solution, composed by 6% $FeCl_3$ and 1% HCl, is more aggressive in comparison to artificial seawater, since the measured CPTs in this solution are lower than in artificial seawater. Nevertheless, the tendency is kept and the difference in the pitting resistance between the two alloys is even more pronounced.

The next step is then to have both alloys tested according to ASTM G61 in artificial seawater. The cyclic potentiodynamic polarization curves measured at 30 °C are shown on Figure 7. The measured pitting-potential (E_{pit}) and pitting-current density (i_{pit}) are summarized on Table 7.

At 30 °C, there is no significant difference that can be observed between both alloys. The reason why there is no significant difference seen can be understood based on the Avesta-cell results that show that, at 30 °C, in artificial seawater, both alloys are resistant to localized corrosion. The current increase, which indicates corrosion activity, only starts to increase after this temperature. Therefore, it is expected that, at a temperature of at least 40 °C we would be able to see a different behavior between the two materials.

Nevertheless, it is important to mention that, in artificial seawater, the current density at which the applied potential reverses to the negative direction must be set much lower for UNS N08825. During the experiments, it was observed that this material tends to corrode much faster when the pitting potential is achieved and crevice corrosion initiates. Because the reduction of reverse current density was only applied for UNS N08825, the repassivation potentials of both alloys can not be compared. Applying a potential to higher values and longer times leads to the development of more severe and stable pits, which are likely to destabilize the passive layer. Thereby, the repassivation is more challenging.
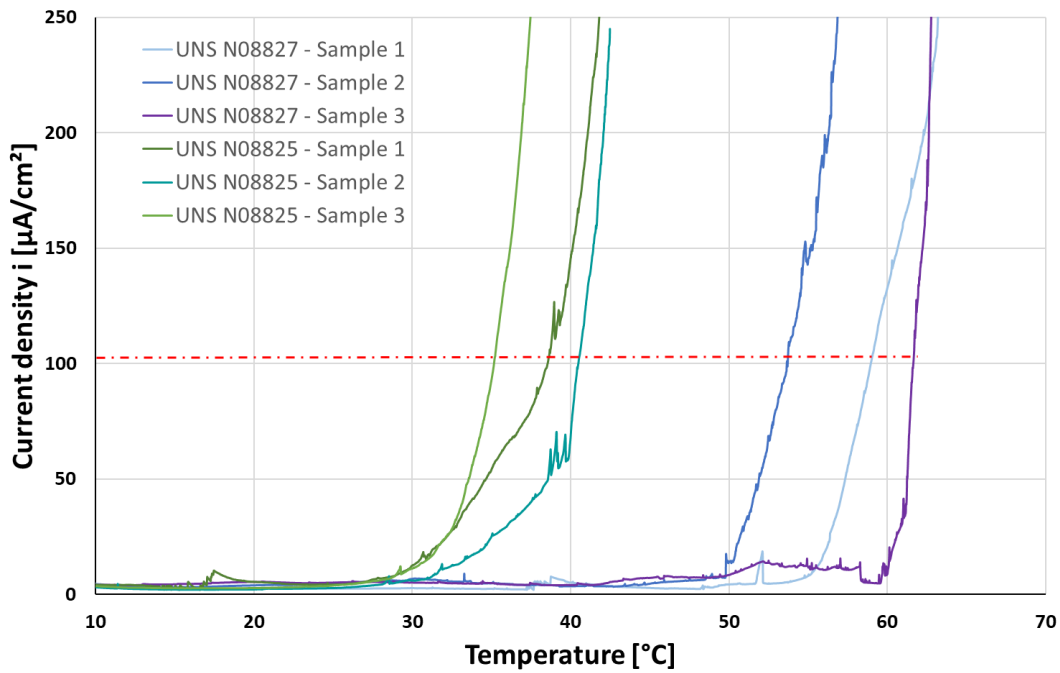
Figure 6: Current density measurements of UNS N08825 and UNS N08827 during temperature increase under synthetic seawater according to ASTM G150
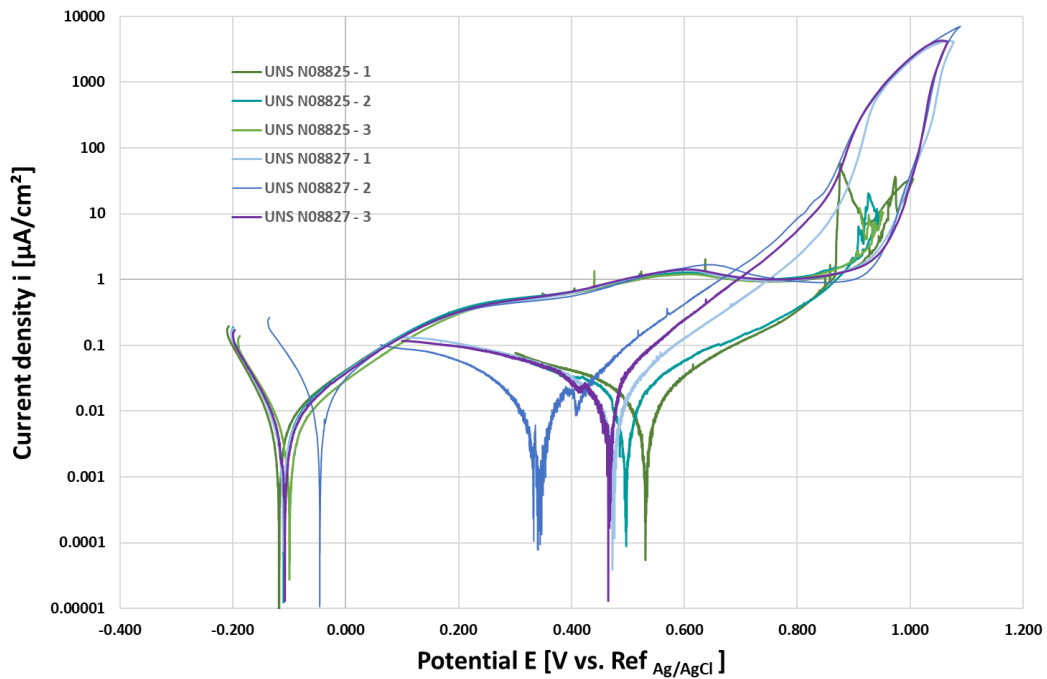

Figure 7: Cyclic potentiodynamic polarization curves of UNS N08825 and UNS N08827 in artificial seawater measured according to ASTM G61 at 30 °C

Table 7: Pitting potential and pitting corrosion at 30 °C defined based on cyclic-pontentiodynamic polarization curves in artificial seawater according to ASTM G61.

Alloy	Sample	E_{pit} [$V_{(Ag/AgCl)}$]	i_{pit} [$\mu A/cm^2$]
UNS N08825	1	0.930	2.500
	2	0.908	2.310
	3	0.894	1.768
	Average	**0.911 ± 0.015**	**2.193 ± 0.31**
UNS N08827	1	0.929	1.428
	2	0.921	1.854
	3	0.925	1.722
	Average	**0.9 ± 0.003**	**1.7 ± 0.178**

CONCLUSIONS

Based on the data presented, the following conclusions could be taken:
- The acidified iron-chloride solution used to perform ASTM G48 immersion tests is more aggressive than artificial seawater with chemical composition according to ASTM 1141 in terms of localized corrosion for the alloys addressed by this paper.
- UNS N08827 shows a higher critical pitting temperature in both acidified iron-chloride solution and artificial seawater in comparison to its precedent alloy, UNS N08825, making possible the use of UNS N08827 in applications at which the material is exposed to higher temperatures.
- During the cyclic potentiodynamic tests at a temperature of 30 °C, no significant difference can be seen in the behaviors of both alloys in artificial seawater and in acidified iron-chloride solution. A different behavior is expected at higher temperatures and tests are going to be repeated.

Since this test program has been carried out in laboratory using artificial seawater, the effect of microbiological corrosion has not been approached. Additional investigations are going to be carried out to evaluate the aspect of microbiological corrosion as well.

ACKNOWLEDGEMENTS

REFERENCES

1. International, ASTM. ASTM B424-19 Standard Specification for Nickel-Iron-Chromium-Copper Alloys Plate, Sheet and Strip. 2019.
2. S. Thompson, J. McIntyre. Special Metals Corporation: Innovator of the future celebrates 100 years of excellence. s.l. : Stainless Steel World, May 2006.
3. J. Botinha, M. Wolf, B. Gehrmann, H. Alves. "Alloy UNS N08827: a New and Sdvance Version of Alloy UNS N08825 with Better Corrosion and Hot Cracking Resistance". Houston, TX : NACE Corrosion 2021, 2021. C2021-16398.
4. V. Shankar, T.P.S. Gill, A.L.E.Terrance, S.L. Mannan and S. Sundaresan. Relation between Microstructure, Composition, and Hot Cracking in Ti-Stabilized Austenitic Stainless Steel Weldments. s.l. : Metallurgical and Materials Transactions A, Volume 31 A, p. 3109-3122, 2000.
5. Lipporld, J.C. An Investigation of Weld Cracking in Alloy 800. s.l. : Welding research supplement, p. 91-103, March 1984.

6. J. Botinha, M. Wolf, H. Alves. On the weldability and corrosion resistance of alloy UNS N08827 - a further improvement of alloy UNS N08825. Denver, Colorado : AMPP, 2023.

7. ASTM G48 - 11 Standard Test Methods for Pitting and Crevice Corrosion Resistance of Stainless Steels and related Alloys by Use of Ferric Chloride Solution. s.l. : ASTM International. West Conshohocken, United States, 2015.

8. U. Heubner, et al. Nickel Alloys and high-alloyed special stainless steels, 4th edition. s.l. : Renningen, Germany: Expert-Verlag, 2012.

9. ASTM D1141-52: Standard Specifications for Substitute Ocean Water. s.l. : (West Conshohocken, PA: ASTM International).

10. ASTM G150-18: Standard Test Method for Electrochemical Critical Pitting Temperature Testing of Stainless Steels and Related Alloys. s.l. : (West Conshohocken, PA: ASTM International), 2018.

11. [Online] 02. 11 2023. https://www.gamry.com/cells-and-accessories/electrochemical-cells/flexcell-critical-pitting-temperature-cell-kit/#:~:text=The%20Flexcell%E2%84%A2%20(Part%20No,seal%20can%20be%20seen%20below..

12. *ASTM G61 - 86(2018): Standard Test Method for Conducting Cyclic Potentiodynamic Measurements for Localized Corrosion Susceptibility of Iron-, Nickel-, or Cobalt-Based Alloys.* s.l. : (West Conshohocken, PA: ASTM International), 2018.

13. J. Botinha, M. Wolf, B. Gehrmann, H. Alves. Alloy UNS N08827: a New and Advanced Version of Alloy UNS N08825 with Better Corrosion and Hot Cracking Resistance. s.l. : AMPP. Houston, TX., 2021. C2021-16398.